EUROfusion

WPSAE-CPR(17) 18387

A. von der Weth et al.

Methodology to evaluate hydrogen isotopes diffusivities and permeabilities from experiments with a purged permeator setup

Preprint of Paper to be submitted for publication in Proceeding of 13th International Symposium on Fusion Nuclear Technology (ISFNT)

This work has been carried out within the framework of the EUROfusion Consortium and has received funding from the Euratom research and training programme 2014-2018 under grant agreement No 633053. The views and opinions expressed herein do not necessarily reflect those of the European Commission.

This document is intended for publication in the open literature. It is made available on the clear understanding that it may not be further circulated and extracts or references may not be published prior to publication of the original when applicable, or without the consent of the Publications Officer, EUROfusion Programme Management Unit, Culham Science Centre, Abingdon, Oxon, OX14 3DB, UK or e-mail Publications.Officer@euro-fusion.org

Enquiries about Copyright and reproduction should be addressed to the Publications Officer, EUROfusion Programme Management Unit, Culham Science Centre, Abingdon, Oxon, OX14 3DB, UK or e-mail Publications.Officer@euro-fusion.org

The contents of this preprint and all other EUROfusion Preprints, Reports and Conference Papers are available to view online free at http://www.euro-fusionscipub.org. This site has full search facilities and e-mail alert options. In the JET specific papers the diagrams contained within the PDFs on this site are hyperlinked

Methodology to evaluate hydrogen isotopes permeabilities and diffusivities from experiments with a purged permeator setup

Axel von der Weth*, Frederik Arbeiter, Dmitry Klimenko, Volker Pasler, Georg Schlindwein, Kevin Zinn

Karlsruhe Institute of Technology, P.O.Box 3640, D-76021 Karlsruhe, Germany
**Corresponding author: Axel.vonderWeth@kit.edu*

The Q-PETE (Hydrogen Permeation and Transport Experiment) at KIT is set up to investigate hydrogen isotopes permeation through structural materials with specific relevance to the HCPB (helium cooled pebble bed) DEMO blanket breeder zone. The experiment therefore consists of two purged chambers separated by a permeation membrane (made of Eurofer or other steels of interest). The permeated and purged hydrogen is time resolved detected with a mass spectrometer. The experiments are intended to provide validation data for simulation codes. A second objective is the direct determination of material data. The determination of permeation parameters like diffusivity and Sieverts' constants is usually performed by modelling experimental results with a solution of a differential equation, 2nd Fick´s law applied to a flat membrane. Mostly permeation disk or gas release experiments (without purge, measuring the pressure rise) were performed in the past, and according analysis methods were applied.

This paper will introduce necessary methods for purged permeation experiment analysis: A self-developed branch and bound (B&B) algorithm – least square fit algorithm- which will calculate the desired diffusion and Sieverts' constant. The issue of the initial value problem is discussed. Furthermore, a numerically effective approach to handle the signal distortion due to the residence time distribution of the measured gas between the permeation chamber and the analysis station, by re-transformation with a so-called Time Spread Function (TSF), is presented.

Keywords: Hydrogen, permeation, diffusion constant, experiment, analysis, branch and bound algorithm

1. Introduction

Deuterium and tritium are the fuel components of a future fusion power plant. Tritium is generated by neutron irradiation of lithium compounds in the breeder units of the blanket [1]. The knowledge of tritium loses and storage potentials in metallic materials (e. g. EUROFER or 316 L) are necessary for safety issues and to assure tritium self-sufficiency. [2, 3] reports that tritium is transported from the breeding zone by a purge gas system containing He around 1 – 3 bars only about 1 Pa of tritium species mainly HTO, HT and only little less T_2. H_2 is used as additive amounts to several 100 Pa. In contrast nearly all current available permeation literature data [4] is related to pure hydrogen isotopes around 10^5 Pa loading pressure. Mostly a pressure gauge as central measurement device is used.

Therefore the authors are proposing a new kind of hydrogen permeation experiment, where the low pressure side (permeate side) is continuously purged with a hydrogen free sweep gas, so the hydrogen counter pressure on the permeate side is limited to 0.05 - 5 Pa. Such a setup bears the potential to perform experiments also at low loading pressures between 10 - 1000 Pa of hydrogen (Q) relevant to breeder zone conditions. The purged setup however introduces specific problems, which have to be handled in the analysis. This paper publishes the analysis of hydrogen permeation parameters as diffusion- and Sieverts´- constant under conditions specific to purged permeation setups. It is a part of a series of papers about hydrogen permeation in metallic materials, especially reduced activation (9% Cr) steels [4, 5, 6].

2. Q-PETE experimental setup

The proposed new kind of setup is called Q-PETE (Q for hydrogen isotope Permeation Transport Experiment). This setup is described in detail in [5, 6]. Fig 1 displays a simple schematic drawing of the setup reduced to key components. Fig. 2 shows details of the so called permeator. The working principle of the experiment is as follows: A specified hydrogen partial pressure is adjusted on the so called retentate side by continuously supplying an Ar + D_2 mixture. A permeation flux *j(t)* of hydrogen from the retentate side through the membrane to the permeate side will occur. On the permeate side, the permeated hydrogen is mixed with a controlled pure Ar purge flow, and flushed to a quadrupole mass spectrometer (QMS) for quantitative time resolved measurement.

The Q-PETE permeator setup consists of two flanges formed like cups made of 316 austenitic steel, electrically heated in a range 200°C to 600°C. They are separated by a membrane made of the to be investigated material, called specimen**.** This membrane is made from e.g. EUROFER [4] of a thickness w_m of about 1 mm and diameter d_m of about 125 mm. It represents a metallic structure as used for a breeder unit. The two cavities formed by the two cups and the membrane are called retentate chamber and permeate chamber. Copper spring seals (low permeation) are tightening the whole setup. The Q-PETE permeator setup will be mounted in a vacuum tank. The gas inlets in both chambers have

author's email: axel.vonderweth@kit.edu

extensions increasing the inlet surface aiming a pre-heating of both purge gases. The technical realization of Q-PETE is currently on going. The total absolute pressure p_l in retentate chamber is set equal to the permeate chamber pressure p_p. This is a further important advantage to former setups, because no mechanical load (influence on diffusion constant) is applied to the membrane.

Note in usual permeation disk experiments there is a "high" pressure about $p_l = 10^5$ Pa and $x = 1$(Q-concentration), see eq. (2) in the retentate chamber and a low p_p < 0.5 to 10 Pa in the permeate chamber. The pressure increase on the

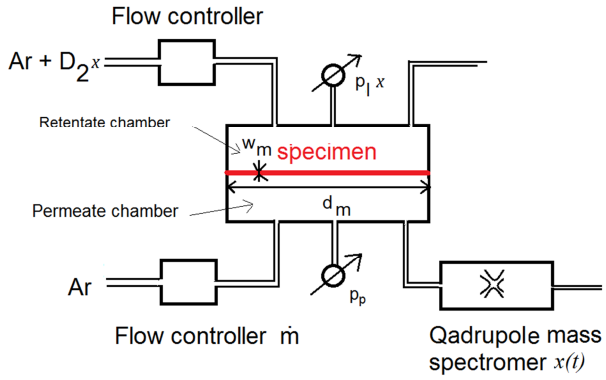

Fig 1: Schematic flow instrumentation drawing of a purged permeator setup

permeate side during a permeation disk experiment generates systematic errors from a non-vanishing Q-concentration.

The deuterium (possibly other hydrogen species in future) is permeating through the membrane into the permeate chamber with molar flux $j_{meas,i}(t)$ and from there flushed away with pure Ar (molar mass M) with constant mass flow rate $\dot{m}$ to the QMS measuring a concentration $x(t)$, the index i indicates also $t = t_i$ for later discretization:

$$j_{meas,\,i} = \frac{\dot{m}}{M}\; x(t) \qquad (1)$$

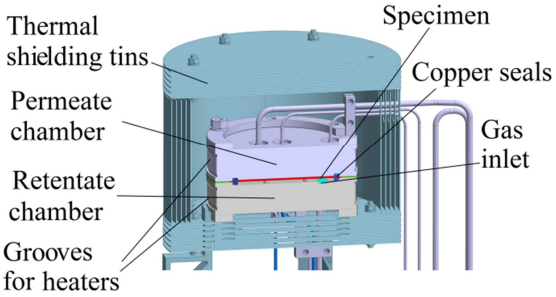

Fig 2: Sketch of the Q-PETE setup.

3. Analysis of Q-PETE experiment

The determination of diffusion constant D_{eff} and the equilibrium Q-concentration $c(0)$ together with Sieverts´ constant K_s

$$c(0) = K_S \sqrt{x\, p_l} \qquad (2)$$

can only be performed by investigating solution of a linear differential equation (Fick´s second law) where D_{eff} enters as parameter and $c(0)$ enters as boundary condition at the interface of Deuterium in the gas phase and Deuterium in the membrane (solid-interstitial-phase). In the permeate chamber a completely vanishing deuterium concentration is assumed by the solution. The fitting solution can be taken from a text book [7, 8].

The third unknown variable t_{off} represents the time shift between start point of measurements (inserting the D_2 into the retentate chamber) and analysis time of the QMS.

$$j_{theo}(t) = \underbrace{\frac{D_{eff}\,c(0)\,d_m^2}{w_m\,4\,\pi}}_{j_{steady\ state}} \left(1 + 2\sum_{k=1}^{\infty}(-1)^k e^{\frac{-k^2\pi^2 D_{eff}\left(t-t_{off}\right)}{w_m^2}}\right) \qquad (3)$$

Note for t- less than t_{off} $j_{thei,\,I}$ is set to zero in eq. (3).

The number of required summands (I_i respectively summation index k) in eq. (3) is clarified by Fig 3. The temperature dependency of D_{eff} is chosen according to, EUROFER (Optifer) conditions data from [10].

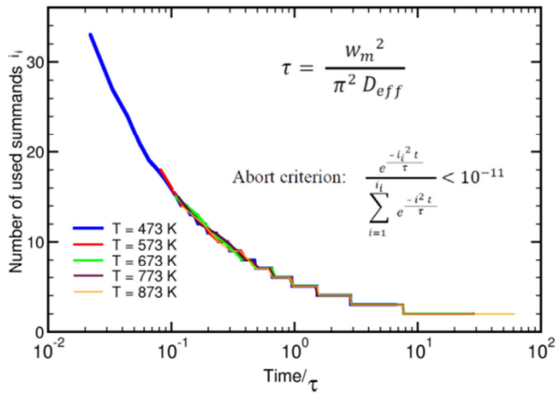

Fig 3: Convergence behavior of eq. (3), note less than 40 terms in the sum are necessary for convergence. The here reported stop criterion is used in further calculations.

Eq. (3) is **one** implicit nonlinear transcendent equation for **three** variables (D_{eff}, $c(0)$ and, t_{off}). So the problem requires (theoretically, without noise, without zero permeation rate) at least three measurement points. But it will not work with three arbitrary points, e.g. think about three points in the steady state where $j_{meas,i}$ is constant. Therefore it is necessary to write how this can be solved by a B&B algorithm using a set of about 200 points (3.1) and also important the determination of initial values (3.2) of B&B.

3.1 The branch and bound B&B algorithm

This section discusses the evaluation of the desired parameters of eq. (3) from experimental results using a B&B algorithm. The key quantity is χ^2 which describes a sum of weighted (relative) standard

deviations for each data point. It is assumed that for minimum χ^2 the set of fitting parameters in eq. (3) for t_{off}, D_{eff} and $c(0)$ represents best estimates.

$$\chi^2 = \frac{1}{n_m - 1} \sum_{i=1}^{n_m} \underbrace{\frac{(j_{theo,i} - j_{meas,i})^2}{(j_{theo,i} + j_{meas,i})^2}}_{\text{"relative deviation"}^2} \qquad (4)$$

Let be n_m the number of measured points where the permeation according to next section (Fig 8) does not vanish (denominator not zero) and note $\chi^2 \geq 0$. It is possible to use the absolute square between measured and theoretical predicted values eq. (4). However this would overweight the "steady state" region in the fitting procedure while the key information is to be extracted from the transient rise regime of j_{theo} , see eq.(9) 3.2 and curvature in fig. 5 (and following).

χ^2 will never be exactly zero due to statistical errors of QMS,

$$\chi^2 \sim \frac{1}{x(t)_{steady,state}} \qquad (5),$$

after finishing of B&B run, systematical errors (leaks, not constant temperature) or discrepancies of the theoretical model vs. experimental or numerical errors. (Excurse: There is no need of observation of numerical error. Increase of the abort criterion to10^{-3}, Fig. 3, shifts χ^2 to 10^{-6} and the error of D_{eff} and $c(0)$ results to about 2%). But in this case the algorithm finds a solution for the parameters (also called var) with less as possible error which is adequate.

For each parameter the B&B algorithm sets up two variants. The first variant uses the current value of the parameter, the second variant is calculated with a slightly changed value (increment by ε) of the same parameter. The parameter from the variant with lower χ^2 will serve as initial value for the next iteration step and so on.

t_{off} is the first variable to be treated in the first step of B&B algorithm: The algorithm is (time) shifting the permeation function “to the right”. It recognizes by a lowering of χ^2 that it is changing in the right direction. As soon as χ^2 sarts to increase, it has to go “back”, by changing the sign of ε and reducing the amount of ε *by* a factor 0.5. The amount of ε falls under a specific limit and the step is finished. The search for a fitting solution of eq, (3) has been changed to a minimization problem.

The limits for ε are given by a $t_{off} \cdot 0.2/ik$ and $t_{off} \cdot 0.01/ ik$ where t_{off} is initialized in 3.2 and $ik < 1000$ the number of current super cycle. A super cycle contains at least three steps corresponding to three variables where each of the desired parameters is sequential treated up to the lower limit of ε. This concept of steps and super cycles turned out most effective. The algorithm starts with coarse steps for quickly approaching a quite good result (small super cycle number) and finer steps (smaller ε) improving a better result at higher super cycle number.

It is also necessary to observe the lowest and the highest value of χ^2 eq.(4) during all super cycles. It is a stop criterion for the algorithm when there is a vanishing difference between both values any more, see later Fig 7, this is a sign that the algorithm has been found an end.

But additional these values are greater than 10^{-3}, it will indicate, that there is an error. Wrong initial values or the experimental conditions need improvement, see later Fig 7.

The D_{eff} (step two) and $c(0)$ (step three) variants are chosen in the same different way to t_{off}:

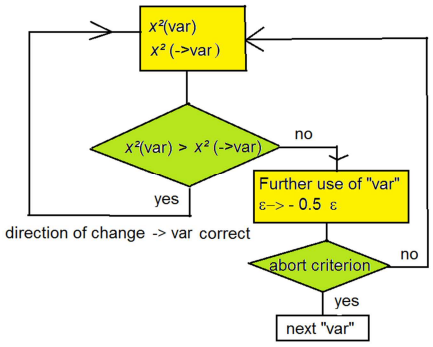

Fig 4: Diagram of one step of the used B&B algorithm.

$$D_{eff} \rightarrow D_{eff}(1 + \epsilon) \qquad (6)$$

ε is chosen by eq. 7 ($1 \geq tolerance \geq 10^{-3}$).

$$\frac{0.3}{ik + 0.01\, ik^2} \geq |\varepsilon| \geq \frac{tolerance}{ik^2 + 2\, ik} \qquad (7)$$

This procedure owns the large advantage that the desired variables D_{eff} and $c(0)$ will be always positive and the progress to small values of these variables is in a fitting way (note an artificial constant $\varepsilon = -0.1$ creates a geometrical serial) to the B&B algorithm. The influence of the permeation curve is displayed by Fig 5. Note, in later super cycles of B&B algorithm $j_{steady\ state}$ is possibly not fulfilled by current D_{eff} and $c(0)$ value, see eq. (10).

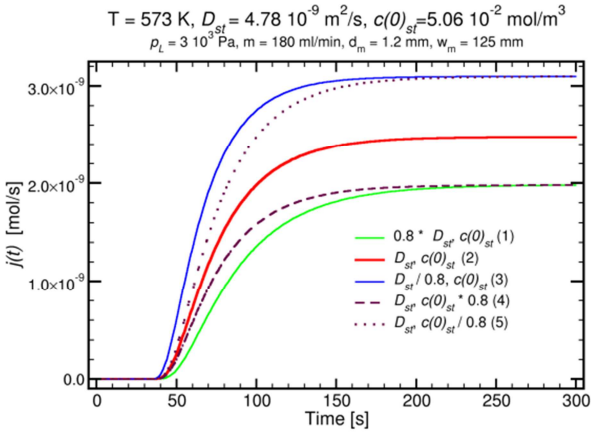

Fig 5: This diagram illustrates the influence of “wrong” diffusion and $c(0)$ constants, note a smaller D_{eff} lowers the curvature of the permeation graph and $j_{steady\ state}$. In contrast a smaller $c(0)$ lowers only $j_{steady\ state}$.

There is also a Gaussian algorithm available without bounds, but here one step is added to B&B algorithm with an advantage of bounds: Step 4 is influencing only the curvature of the permeation graph and keeping

constant $j_{steady\ state}$ as bound. The influence of the step 4 algorithm can be seen by comparison of graph 1 with 5 and graph 3 with 4 of Fig 5: It changes together (ϵ according eq. 7):

$$D_{eff} \rightarrow D_{eff} \cdot (1 + \epsilon) \text{ and } c(0) \rightarrow c(0)/(1 + \varepsilon) \quad (8)$$

Fig. 6 indicates expected quality of curve fitting with the B&B algorithm. It shows "simulated" experimental results generated with eq. (3) (green thick curve) together with B&B algorithm fitting results that should recover the original D_{eff} and *c(0)* values by bad initial values (see **3.2**, indicated by the factor 80 and 0.5 in Fig 6 and 7 are used with and without step 4 eq. (8). The dashed red line of Fig 7 shows that the results fully matching, while the maroon dashed line demonstrates a bad working B&B algorithm.

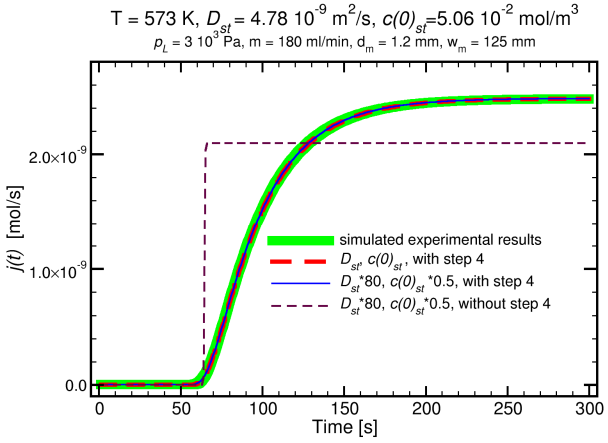

Fig 6: Results of B&B algorithm with and without step 4 (brown dashed), additional bad initial values.

But yet only the use of step 4 (constraints) is improving the result to the blue straight line also seen by the corresponding Fig 7 for ^{2} . The use of proper (3.2) initial values is improving the rate of convergence and quality of results. Typical B&B error values for a correct working algorithm are less than 0.01 % for D_{eff} and *c(0)* .

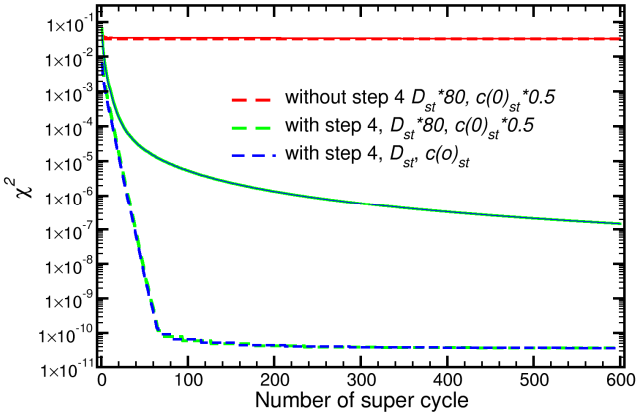

Fig 7: Convergence of in Fig 6 displayed results of B&B algorithm, dashed lines indicate the lower value of both χ^2values.

3.2 Determination of starting values

Above the need of "effective" initial values for the B&B algorithm was demonstrated. Using the first term of the sum in eq. (3) yields the initial value for D_{eff}:

$$D_{eff} = \frac{w_m^2}{\pi^2 \Delta t_d} \quad (9)$$

The desired time interval Δt_d can be evaluated from the interval of that time point were $j_{meass,\ I}$ reaches a half of $j_{steady\ state}$ and the time where the permeation reaches *(0.5+0.34)** $j_{steady\ state.}$.

$$c(0) = \frac{j_{steady\ state}\, w_m\, 4}{D_{eff}\, d_m^2\, \pi} \quad (10)$$

A view to eq. (3) yields the initial value for *c(0)* (10), D_{eff} is taken from eq. (9).

Now the initial value for t_{off} will be determined by that time point, by that reaches $j_{meas,\ I}$ a half of $j_{steady\ state}$ and Δt_d is subtracted from the former point. These initial values are generating the green dashed line in Fig 8 as a first approximation of the experimental observed results (note time shift), displayed as blue line und the B&B solution displayed as red line in Fig 8

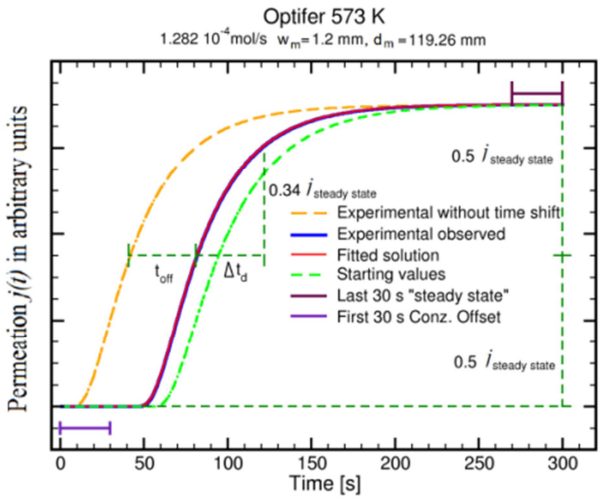

Fig 8: Explanation graphics for initial values, a possible zero offset is subtracted from all measured permeation values.

3.3 The Time Spread Function (TSF)

According to Fig 1 the Q-containing Ar is transported from the chamber to QMS. Hydraulic (flow profile related) and inter diffusive transport leads to a dispersion and a lag between the *j(t)* signals over the membrane and at the QMS respectively (See [5] for details). The dispersive effects between two neighboring fluid elements (i.e., in a pipeline) could be generalized by a diffusion-like equation and discretized this with a chain of bucket elements (Bucket Chain Model BCM) [11], where the bulk convective transport and superimposed dispersion is modeled. Between neighboring buckets exists "diffusive" exchange, meaning an amount of gaseous Q-atoms is moving depending on concentration difference between adjacent buckets maintaining mass conservation of Q.

The red curve in Fig 9 illustrates the thus distorted signal giving an impression what errors are generated: The

original signal is shared and the slope reduced. Case the D_{eff} result is reduced by a factor of 0.5, the *c(0)* result will be enhanced by a factor of two. The so called TSF

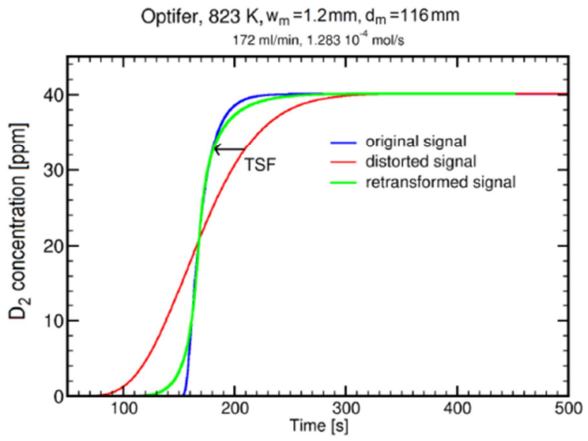

Fig 9: Distorted graph in red by BCM and retransformation by TSF in green. Note here concentration in mass spectrometer is displayed.

indicates the time shift (black arrow in Fig 9) in which direction of the time axis the current point in the relative permeation has to be moved. The green graph - the by TSF retransformed signal- tells the success compared with the non-disturbed signal shown as blue graph.

An experimental TSF curve can be determined by use of two flow controller (one for pure Ar and an other for Q-mixed Ar e.g. 1000 ppm) in the inlet of the rentate chamber, mixing the gas in the time dependent ratio fulfilling according eq. (3). The specimen has to be replaced by a micro porous specimen. This procedure has to be performed for each to be investigated temperature and purge gas flow rate caused by temperature dependency of gas diffusion. Fig 10 shows an "average" TSF with TSF equation in the graphics.

An approach easily accessible in practice to determine a TSF for an experimental setup is computational fluid dynamics, with appropriate models for convective, diffusive and - if applicable - turbulent transport. In our class of problems, the flow is laminar, so only a minimum of assumptions has to be introduced into the flow modeling

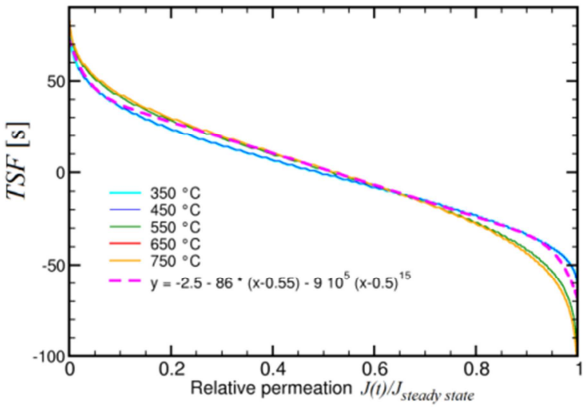

Fig 10: Used TSF for Fig 11

Fig 11 shows the success of fitting TSF: With distortion the "relative deviation", see 3.1. eq. (4) is around 0.5 meaning an error of a factor more than two. Other-wise

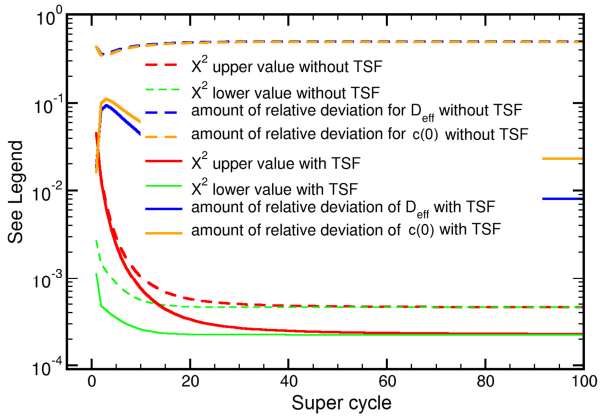

Fig 11: The diagram shows to runs of B&B algorithm firstly without use of TSF and secondly with use of TSF.

firstly TSF according 3.3 is performed, secondly initial values according 3.2 are used and 600 super cycles of B&B algorithm are applied to the data: The success of this analysis is demonstrated by a reduced error of about 1% meaning relative deviation about 0.009 to 0.02. Note Fig 11 displays only the first 100 of 600 super cycles.

4. Remarks on a non-vanishing Q-concentration in the permeate chamber

The here utilized eq. (3) uses a zero Q-concentration in the permeate chamber contrast to a non-vanishing Q-concentration as measurement signal. There are three ways of improving this disadvantage:

Firstly the Ar-mass rate $\dot{m}$ can be increased which lowers the Q-concentration (increasing the noise to signal in the QMS, eq. (5)) in the permeation chamber and then extrapolation of the results for D_{eff} and *c(0)* from experiments dependent on $\dot{m}^{-1}$ to zero Q-concentration, meaning $\dot{m}^{-1} = 0$.

Secondly it is possible to insert non vanishing Q-concentration numerically as subtrahend approximately by square root of the product of Q-concentration *x(t)* multiplied by p_p eq. (2) into eq. (3). The Q-concentration is detected by a mass spectrometer and the pressure is measured by a gauge, see Fig 1.

Thirdly the most precise (but also most computationally expensive) approach would be to generate $j_{theo,\,i}(t)$ as result of a finite differences code which handles the diffusion through the membrane as well as the hydrogen partial pressure buildup in the permeate chamber

5. Conclusion

The current paper publishes an algorithm how a purged permeator experiment Q-PETE is analyzed aiming at a standardized procedure evaluating D_{eff} and *c(0)*. There is no arbitrariness about region of constant permeation rates [7] or e. g. pumping times [9].

For synthetic signals, the algorithm is successful in matching diffusion parameters better than 0.01% deviation.

6 Acknowledgments

This work has been carried out within the framework of the EUROfusion Consortium, and has received funding from the Euratom research and training program 2014-2018 under grant agreement No 633053. The views and opinions expressed herein do not necessarily reflect those of the European Commission

7 References

[1] G. Federici et al., Overview of the design approach and prioritization of R&D activities towards an EU DEMO, Fusion Engineering and Design 109-111 (2016) 1464-1474.

[2] Franza et al., Tritium transport analysis in HCPB DEMO blankets with the FUS-TPC-Code, KIT SCIENTIFIC REPORT 7642, 2013

[3] A. Ciampichetti et al., Conceptual design of Tritium Extraction System for the European HCPB Test Blanket Module, Fusion Engineering and Design 87 (2012) 620–624

[4] A. von der Weth et al., Review of Hydrogen Isotopes Transport Parameters and Considerations to corresponding Experiments, Fusion Engineering and Design (2017), http://dx.doi.org/10.2016/j.fusengdes.2017.04.024

[5] F. Arbeiter et al, Simulations and uncertainty analyses for a hydrogen diffusion experiment using a “two side purged membrane” setup, this conference

[6] D Klimenko et al., Definition of the Q-PETE Experiment for Investigation of Hydrogen Isotopes Permeation through the Metal Structures of a DEMO HCPB Breeder Zone, this conference

[7] K.S. Forcey et al., Hydrogen Transport and Solubility in 316L and 1.4914 Steels for Fusion Reactor Applications, J. Nucl. Mat. 160 (1988) 117-124

[8] J. Crank, The Mathematics of Diffusion, Clarendon Press, Oxford, 1975.

[9] G.A. Esteban et al, Hydrogen Transport and Trapping in EUROFER 97, see “Optifer”, J. Nucl. Mat. 367-370 (2007) 473-477

[10] A. von der Weth, Technical note on Hydrogen permeation parameter in RAFM steel, Karlsruhe 2016, Eurofus. IDM D2MYS5400C, March 2016

[11] F. Arbeiter et al., Development of Tritium Transport Models at BU level for HCPB, final report of WPBB-6.2.2.-2016T, Eurofus. IDM EFDA_D_2MYSSC, Karlsruhe 2016